Ion Implantation Induced Interdiffusion in Quantum Wells for Optoelectronic Device Integration

L. FU, H.H. TAN, M.I. COHEN and C. JAGADISH
Department of Electronic Materials Engineering, Research School of Physical Sciences and Engineering, The Australian National University, Canberra, ACT 0200, Australia

L.V. DAO and M. GAL
School of Physics, University of New South Wales, Sydney, NSW 2052, Australia

NA LI, NING LI, X. LIU, W. LU and S.C. SHEN
Shanghai Institute of Technical Physics, Chinese Academy of Science, Shanghai, China

ABSTRACT

Ion implantation induced intermixing of GaAs/AlGaAs and InGaAs/AlGaAs quantum wells was studied using low temperature photoluminescence. Large energy shifts were observed with proton implantation and subsequent rapid thermal annealing. Energy shifts were found to be linear as a function of dose for doses as high as $\sim 5 \times 10^{16}$ cm^{-2}. Proton implantation and subsequent rapid thermal annealing was used to tune the emission wavelength of InGaAs quantum well lasers as well as detection wavelength of GaAs/AlGaAs quantum well infrared photodetectors (QWIPs). Emission wavelength of lasers showed blue shift whereas detection wavelength of QWIPs was red shifted with intermixing.

INTRODUCTION

Quantum well intermixing has drawn considerable attention in recent years for integration of optoelectronic devices [1-3]. Impurity induced disordering (IID) and impurity free vacancy disordering (IFVD) have been widely used to modify the shape of the quantum wells, in turn their electrical and optical properties [4-7]. However, in the case of impurity induced disordering, residual impurities are detrimental to the performance of devices. In the case of IFVD, defects are produced in the near surface region [8,9] and defect diffusion length should be large enough to reach the quantum wells in the active regions of devices which are often 1-2 micron deep. Ion implantation is a versatile technique and allows introduction of defects in selected regions with defect distribution peaking in the region of interest by choosing appropriate ion energy, dose etc. Recently, ion implantation induced intermixing has been used to tune the emission wavelength of quantum wells and to enhance light emission from V-groove quantum wires [10-12].

In this paper, we review the issues associated with implantation induced intermixing in GaAs/AlGaAs and InGaAs/AlGaAs quantum wells and apply this technique to tune the emission wavelength of quantum well lasers. Intermixing has also been used to tune the detection wavelength of quantum well infrared photodetectors.

EXPERIMENTAL

The GaAs/AlGaAs, InGaAs/GaAs and InGaAs/AlGaAs quantum well structures and InGaAs quantum well laser structures used in this study were grown by metal organic vapor phase epitaxy (MOVPE) on semi-insulating and n+-GaAs (100) substrates, respectively. Quantum well infrared photodetector structures were grown by molecular beam epitaxy on semi-insulating (100) GaAs substrates. Proton irradiation was carried out at room temperature using 40 keV Protons for quantum well structures, 220 keV protons for laser structures and 900 keV proton for QWIP structures. Proton energies for quantum well and laser structures were chosen to locate the peak of the defect profile closer to the quantum wells. In the case of QWIPs, peak of the damage profile is located in the substrate and tail of the profile is used to create uniform distribution of damage in the quantum well region consisting of 50 quantum wells doped with silicon. Half of each sample was masked during irradiation to serve as a reference region and sample was tilted 7° off the beam axis to minimise channeling effect. Rapid thermal annealing was carried out in argon ambient at temperatures in the range of 900-950°C for periods of 30-60 sec. Low temperature (12K) photoluminescence (PL) was performed to monitor energy shifts in quantum wells due to interdiffusion using green He-Ne laser (543.5 nm) as the excitation source and the luminescence was detected with a silicon CCD through a monochromator.

RESULTS AND DISCUSSION

GaAs/AlGaAs Quantum Wells

A four quantum well structure of GaAs/Al$_{0.54}$Ga$_{0.46}$As with nominal quantum well thicknesses of 1.4 nm, 2.3 nm, 4.0 nm and 8.5 nm was implanted with 40 keV protons in the dose range of 1×10^{14} to 5×10^{16} cm^{-2}. Samples were rapid thermally annealed at 900°C for 60 sec. Photoluminescence measurements showed blue shift of the emission peak for doses above 5×10^{14} cm^{-2}. Energy shifts were linear with proton dose to 5×10^{16} cm^{-2} for all the quantum wells. Energy shifts as large as 200 meV were obtained without significant degradation in the PL intensity (only a factor of two lower in intensity), suggesting that proton implantation is quite effective in achieve quantum well intermixing. Results of these studies [10,11] were used to design experiments to tune detection wavelength of GaAs/AlGaAs QWIPs.

InGaAs/AlGaAs Quantum Wells

The InGaAs/GaAs and InGaAs/AlGaAs structures consisted of two quantum wells of 5 nm thickness with In$_{0.15}$Ga$_{0.85}$As and In$_{0.30}$Ga$_{0.70}$As well and GaAs and Al$_{0.2}$Ga$_{0.8}$As barriers, respectively. Proton irradiation was carried out at room temperature using 40 keV protons. Rapid thermal annealing was carried out in argon ambient at 900°C for 60 sec. The PL spectra from InGaAs/GaAs and InGaAs/AlGaAs samples implanted at doses of 1×10^{15} cm^{-2} and 5×10^{15} cm^{-2} are shown in Fig. 1(a) and 1(b), respectively. It can be seen that the proton irradiation and subsequent rapid thermal annealing led to blue shift of the emission wavelength from all the quantum wells. PL intensity decreased with increase in ion dose in InGaAs/GaAs samples indicating that the non-radiative recombination centers introduced by proton implantation are not removed by RTA. However, PL intensity recovery was very good (>50%) for InGaAs/AlGaAs

quantum wells and this is attributed to the dynamic annealing of defects during ion irradiation. Previous studies proposed that the presence of AlGaAs offers some protection against damage accumulation in adjacent GaAs regions due to the strong dynamic annealing of the mobile point defects generated in AlGaAs [13,14]. Accordingly, for InGaAs QW sandwiched between AlGaAs barrier layers, it is possible that during implantation a similar process might occur. This together with the simultaneous dynamic annealing in the AlGaAs layers, preventing the formation of large defect clusters, suggests that the residual defects in the sample would be predominantly point defects. These point defects have lower thermal stability and are annealed much more easily than defect clusters (in the case of InGaAs/GaAs QWs) to promote intermixing and hence the remarkable recovery of the PL intensities of the InGaAs/AlGaAs samples.
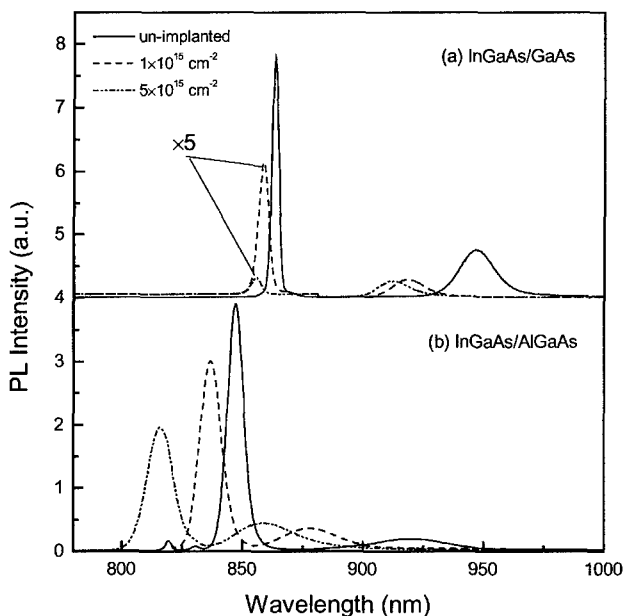

Fig. 1   Comparison of PL spectra for InGaAs QW samples with GaAs or AlGaAs barriers after proton implantation with doses of 1×10^{15} cm^{-2}, 5×10^{15} cm^{-2} and RTA at 900°C, 60s. The peaks from the $In_{0.15}Ga_{0.85}As$ QWs of the implanted InGaAs/GaAs samples are multiplied by a factor of 5 in order to make clearer comparison.

Quantum Well Lasers

A standard graded-index separate confinement heterostructure (GRINSCH) laser with active region consisting of 7 nm $In_{0.2}Ga_{0.8}As$ quantum well sandwiched by 12 nm $Al_{0.2}Ga_{0.8}As$ barriers was grown by MOVPE. Laser structure was irradiated with 220 keV protons to locate the damage peak nearer to the quantum well region. Half of the sample was masked (for reference) and the other half was irradiated with a dose of $1x10^{15}$ cm^{-2} and the whole sample was annealed at 900°C for 30 sec. After RTA, these samples, together with as-grown samples were fabricated into 4 micron stripe width ridge waveguide lasers by optical lithography. Figure 2 shows the laser spectra from three different devices (as-grown, as-grown and annealed, proton implanted and annealed) at 1.5 I_{th} under pulsed conditions using 2 microsec pulses of 5% duty cycle at room temperature. Wavelength shifts of 30 nm and 49 nm (compared with as-grown sample) were obtained from the reference annealed sample and irradiated and annealed sample, respectively.
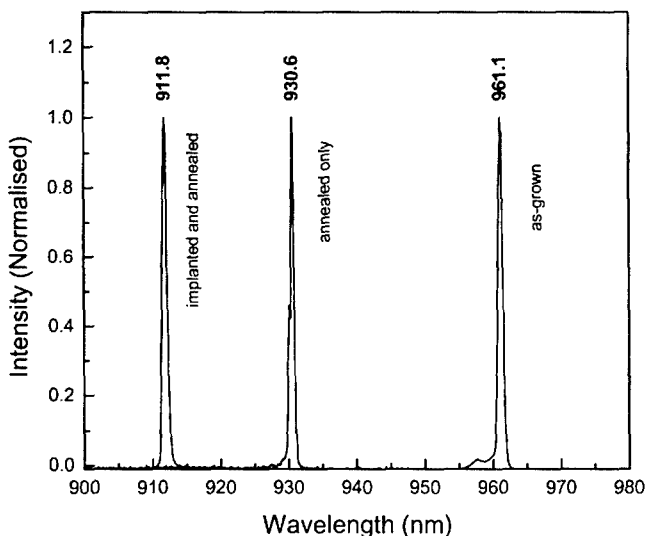

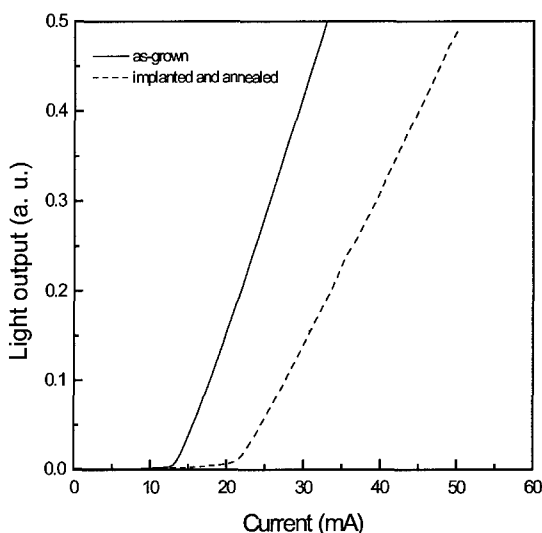Fig. 2   Lasing spectra for the InGaAs/AlGaAs lasers before and after H implantation measured at room temperature.

Fig. 3 *L-I* curves for the InGaAs/AlGaAs lasers (length of ~ 710 μm) before and after H implantation measured at room temperature.

Figure 3 shows L-I curves of the InGaAs/AlGaAs lasers measured at room temperature before and after H implantation and annealing. Though threshold current has increased in implanted and annealed samples, slope efficiency is similar that of the as-grown lasers suggesting that the laser quality is not significantly degraded due to proton implantation and annealing. Increase in threshold current is mainly due to the presence of non-radiative recombination centers. Further optimisation of implantation and annealing conditions could lead to reduction in non-radiative recombination centers. This suggests that the ion irradiation induced intermixing is a promising technique for integration of lasers operating at different wavelengths on the same chip.

Quantum Well Infrared Photodetectors.

Proton implantation and rapid thermal annealing was used to tune the detection wavelength of quantum well infrared photodetectors. The structures used in this work were n-type GaAs/AlGaAs bound to continuum QWIPS grown by molecular beam epitaxy on semi-insulating substrates. The structure contained 50 quantum wells sandwiched between 2 um top and 1.3 um bottom contact n+-GaAs layers. The quantum wells were nominally 4.5 nm Si doped (~10^{18} cm^{-3}) GaAs with 50nm undoped $Al_{0.3}Ga_{0.7}As$ barriers. In order to obtain homogeneous intermixing in the quantum well region, 900 keV protons were chosen and the damage peak was located

in the substrate and a relatively uniform distribution of displacements across the quantum well region was achieved. During implantation, part of the sample was masked to serve as a reference and the rest of the sample was implanted with doses in the range of $1\text{-}4\times10^{16}\text{cm}^{-2}$. All the samples were rapid thermally annealed at 950°C for 30sec under argon ambient. QWIPs were processed into 250x250 um^2 devices using standard lithography and wet etching. A 6 micron period grating was etched to allow normal incidence operation.

The spectral responses from all the samples acquired at 80K using Fourier transform infrared spectrometer are shown in Fig. 4. The peak detection wavelength has shifted from 6.8 microns for the unimplanted reference sample to 7, 7.3, 7.6 and 8.6 microns for samples implanted with doses of 1, 2, 3, 4 $\times10^{16}$ cm^{-2}, respectively. The dark current measurements have shown that the dark current increased by one to two orders of magnitude with increase in ion dose. This could be due to changes in the potential profile of the quantum well due to interdiffusion as well as due to the presence of residual defects which enhance tunneling probability of electrons. The contribution of residual defects to dark current could be reduced by carrying out multiple implant-anneal sequences [15,16].
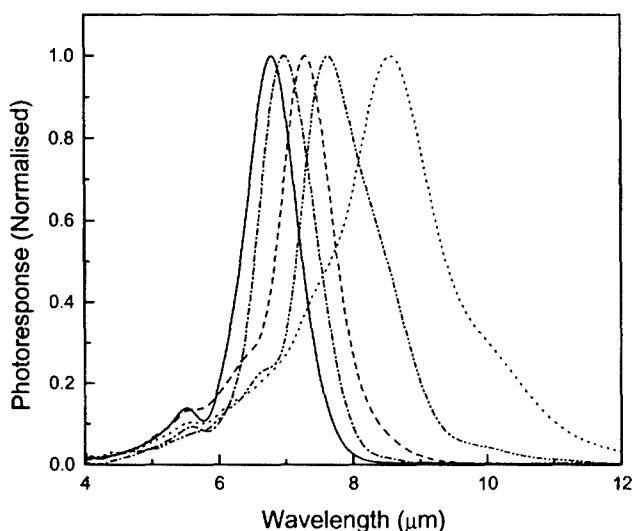

Fig. 4   Normalised photoresponse for the un-implanted sample and samples implanted with the doses of 1, 2, 3, 4×10^{16} cm^{-2} (from left to right) by a single high energy measured at 80 K under the bias of -6 V.

CONCLUSIONS

Proton implantation and rapid thermal annealing was used to create interdiffusion in GaAs/AlGaAs quantum wells leading to blue shift in the emission wavelength of the quantum wells. Blue shift in the emission wavelength of InGaAs quantum well lasers was achieved with modest degradation in device performance. In the case of quantum well infrared photodetectors, a red shift was obtained. In summary, suitability of implantation induced interdiffusion for optoelectronic device integration was demonstrated by fabricating multi-wavelength quantum well lasers and quantum well infrared photodetectors.

References

1. D.G. Deppe and N. Holonyak, Jr., J. Appl. Phys., 64, R93 (1988).
2. E.H. Li, Ed. Quantum Well Intermixing for Photonics, SPIE Milestone Series, Bellingham, WA, 1997
3. E.H. Li, Ed. Semiconductor Quantum Well Intermixing, Gordon and Breach, Amsterdam, 2000
4. Shu Yuan, C. Jagadish, Yong Kim, Y. Chang, H. H. Tan, R. M. Cohen, M. Petravic, L. V. Dao, M. Gal, M. C. Y. Chan, E. H. Li, J. S. O, and P. S. Zory, IEEE Journal of Special Topics in Quantum Electronics 4, 629-635 (1998).
5. P.N.K. Deenapanray, H.H. Tan, M.I. Cohen, K. Gaff, M. Petravic and C. Jagadish, J. ElectroChem. Soc. 147, 1950-1956 (2000).
6. P.N.K. Deenapanray and C. Jagadish, J. Vac. Sci. Technol. B 19, 1962-1966 (2001).
7. L. Fu, P.N.K. Deenapanray, H.H. Tan, C. Jagadish, L.V. Dao and M. Gal, Appl. Phys. Lett. 76, 837-839 (2000).
8. R.M.Cohen, G. Li, C. Jagadish, P.T. Burke and M. Gal, Appl. Phys. Lett. 73, 803-805 (1998).
9. P.N.K. Deenapanray, H.H. Tan, C. Jagadish and F.D. Auret, Appl. Phys. Lett. 77, 696-698 (2000).
10. C. Jagadish, H.H. Tan, S. Yuan and M. Gal, Mater. Res. Soc. Symp. Proc. 484, 397-411 (1998).
11. H.H. Tan, J.S. Williams, C. Jagadish, P.T. Burke and M. Gal, Appl. Phys. Lett. 68, 2401-2403 (1996).
12. Y. Kim, S. Yuan, R. Leon, C. Jagadish, M. Gal, M.B. Johnston, M.R. Phillips, M.A. Stevens Kalceff, J. Zou and D.J.H. Cockayne, J. Appl. Phys. 80, 5014-5020 (1996).
13. H.H. Tan, J.S. Williams, C. Jagadish, A. Skirowski, Z. Jin and D.J.H. Cockayne, J. Appl. Phys. 77, 87-94 (1995).
14. H.H. Tan, C. Jagadish, J.S. Williams, Z. Jin, D.J.H. Cockayne and A. Skirowski, J. Appl. Phys. 80, 2691-2701 (1996).
15. L. Fu, H. H. Tan, C. Jagadish, Na Li, Ning Li, X. Q. Liu, W. Lu, and S. C. Shen, Appl. Phys. Lett. 78, 10-12 (2001).
16. L. Fu, H.H. Tan, C. Jagadish, Na Li, N. Li, X. Liu, W. Lu and S.C. Shen, Infrared Phys. & Technol. 42, 171-175 (2001).